Supporting Information

Millet and Whittaker 10.1073/pnas.1407087111

SI Materials and Methods

Plasmids and Viruses. Influenza virus strain A/WSN/1933(H1N1) HA-encoding and neuraminidase-encoding (NA-encoding) plasmids, pEF4-WSN-HA and pEF4-WSN-NA, were described previously (1).

Embryonic chicken egg-passaged recombinant influenza virus strain A/WSN/1933(H1N1) was generated as described previously (1).

Sequence Analysis of MERS-CoV S1/S2 and S2′ Sites. Coronavirus S protein sequence alignments were performed using ClustalX 2.1 software with the following sequences: FCoV-RM (ACT10854.1), FCoV-1146 (YP_004070194.1), MERS-CoV EMC/2012 strain (AFS88936.1), BatCoV-HKU4 (YP_001039953.1), SARS-CoV (NP_828851.1), HCoV-HKU1 (AAT98580.1), MHV-JHM (YP_209233.1), IBV-Beaudette (NP_040831.1), IBV-M41 (AAW33786.1), and IBV-Cal99 (AAS00080.1). Sequences were scored for their predicted cleavability by furin using the PiTou 2.0 software package (2); (www.nuolan.net/reference.html). A negative score indicates a sequence not predicted to be cleaved by furin, whereas a positive score denotes prediction of furin cleavability. Fluorogenic [(7-methoxycoumarin-4-yl)acetyl/2,4-dinitrophenyl (MCA/DNP) fret pair] 10-mer peptides derived from MERS-CoV and BatCoV-HKU4 S S1/S2 and S2′ sites were synthesized by RS Synthesis. Purified recombinant human furin was purchased from New England Biolabs. For each reaction, 1 unit enzyme was used in a 100-μL reaction volume of buffer containing 100 mM Hepes, 0.5% Triton X-100, 1 mM $CaCl_2$, and 1 mM 2-mercaptoethanol, with each peptide diluted to 50 μM. Reactions were performed at 30 °C, and fluorescence emission was measured with a SpectraMax fluorometer (Molecular Devices), enabling determination of V_{max}.

siRNA and Inhibitors. The inhibitor dec-RVKR-CMK was used to inhibit furin (Tocris Bioscience), with cells treated 2 h before infections at doses varying from 0 to 100 μM, depending on the experiment, and with DMSO used as vehicle control. Treated cells were monitored daily for cytotoxicity, with no obvious signs or detachment of cells observed even at the highest concentrations of inhibitor. Cathepsin B (CA-074Me) and L (cathepsin L inhibitor III) inhibitors were obtained from Calbiochem, and camostat (TMPRSS inhibitor) was purchased from Sigma-Aldrich. Cathepsin inhibitors and camostat were used at a concentration of 25 μM, either alone or with furin inhibitor. For endosome acidification blockade, NH_4Cl (J.T. Baker) and concanamycin A (Fluka–Sigma Aldrich) were used with a 2-h treatment of cells before infection. To silence furin expression, an equimolar mix of siRNA duplexes specifically targeting human furin sequences (J-005882-05, J-005882-06, J-005882-07, and J-005882-08) were used (ThermoScientific). For nontargeting controls, the siGENOME Non-Targeting #3 siRNA was used (ThermoScientific). Transfections of siRNAs were performed using the Dharmafect siDuo transfection reagent according to the manufacturer's instructions (ThermoScientific). To enhance siRNA knock-down, 48 h after the first transfection, a second round of transfection was performed for another 48 h, after which time cells were used for pseudovirion infection.

Western Blot Analyses. For analysis of MERS-CoV S cleavage fragments, 10^6 HEK-293T cells were seeded in six-well plates. The cells were transfected with MERS-CoV S wt- or mutant-encoding plasmids using the Lipofectamine 2000 transfection reagent according to the manufacturer's guidelines (Life Technologies), with or without cotransfection of furin-encoding plasmid or furin inhibitor treatment. The cells were lysed with 1 × radioimmunoprecipitation assay (RIPA) buffer (EMD Millipore) containing protease inhibitor cocktail (Roche). Lithium dodecyl sulfate (LDS) loading buffer and DTT were added to samples, which were then heated at 95 °C for 5 min. Protein samples were separated on NOVEX Bis-Tris gels (Life Technologies) and transferred on polyvinylidene fluoride membranes (GE Healthcare). MERS-CoV S was detected using rabbit polyclonal anti-MERS-CoV-S antibodies generated using recombinant S ectodomain as immunogen (40069-RP02, SinoBiological) and HRP-coupled goat anti-rabbit IgG antibodies (Life Technologies). Detection of Western blot signal was performed using ECL kit from Pierce. Image acquisition was performed using an LAS-3000 imager (FujiFilm).

Pseudovirion Production and Infection. MLV-based MERS-CoV S-pseudotyped or influenza HA-pseudotyped particles (MERSpp/HApp) were generated as previously described (3). HEK-293T cells were cotransfected with MERS-CoV S wt or mutant-encoding plasmids or influenza A/WSN/1933 HA and NA encoding plasmids, along with MLV Gag-Pol packaging construct and the MLV transfer vector encoding luciferase reporter, using Lipofectamine 2000 transfection reagent (Life Technologies) according to the manufacturer's instructions. The cells were incubated at 37 °C 5% CO_2 for 48 h, and supernatants were then harvested and filtered through 0.45-μm membranes. For infection assays, 2.5×10^5 cells were seeded in 24-well plates and incubated at 37 °C for 24 h. The cells were washed with PBS, and 200 μL pseudotyped particles were added to cells and incubated at 37 °C for 2 h. Complete medium was then added and cells were incubated at 37 °C for 72 h, after which luciferase activity was measured using Luciferase Assay Kit (Promega), and luminometer readings performed with a Glomax 20/20 system (Promega). For analysis of S cleavage in MERSpp, pseudotyped particles were ultracentrifuged at 42,000 rpm for 2 h at 4 °C, using a TLA-55 rotor with an Optima-MAX-E centrifuge (Beckman-Coulter). Viral pellets were resuspended in a buffer containing 100 nM Hepes, 0.5% Triton X-100, 1 mM $CaCl_2$, and 1 mM 2-mercaptoethanol. For exogenous furin treatment of pseudovirions, 6 U recombinant human furin were added (New England Biolabs) and proteolytic reaction was performed at 37 °C. Samples were analyzed by Western blot, as described earlier, with detection of MERS-CoV S performed using the rabbit polyclonal antibody 40069-RP02 (SinoBiological) and that of MLV capsid using the mouse monoclonal anti-MLV capsid p30 (4B2, Abcam).

Quantitative RT-PCR. Total RNA from HEK-293T, transfected or not with siRNA, Huh-7, MRC-5, and WI-38 cells, were extracted using the RNeasy Mini Kit (Qiagen) according to the manufacturer's instructions. Concentration of extracted RNA for each sample was measured using spectrophotometric analysis (Quawell), and the 260/280 nm ratio was verified to be between 2.1 and 2.2. Quantitative RT-PCR was performed using the One-Step Quantitect SYBR green kit (Qiagen) with 50 ng total RNA input for each sample. The sequences for the primer sets used for human furin (PrimerBank ID 20336193c1) and human DPP4 (PrimerBank ID 47078262c3) were obtained from the Harvard PrimerBank. Primer sets for human GAPDH (Hs_GAPDH_1_SG) were obtained from Quantitect Primer Assay (Qiagen). Reactions

were performed in 96-well plate format using an Applied Biosystems 7500 Fast Real-Time system. Dissociation curve and threshold cycle analyses were performed with DPP4 and furin expression levels normalized over GAPDH. $2^{-\Delta\Delta CT}$ values were calculated as described previously, with DPP4 and furin expression levels standardized to HEK-293T levels in the case of the differential cell line analysis or to mock siRNA condition for the siRNA assay (4).

Furin Cleavage of S Protein on MERS-CoV Virions. For analysis of furin-mediated S cleavage fragments on MERS-CoV virions, 100 nM Hepes, 0.5% Triton X-100, 1 mM $CaCl_2$, and 1 mM 2-mercaptoethanol was added to viral supernatants, along with recombinant human furin (10 U) (New England Biolabs), and samples were incubated at 37 °C. Furin processing was performed either at neutral or slightly acidic pH (pH 6), and for some samples, incubation of virions with 50 μg/mL soluble recombinant human DPP4 (s-DPP4, Sinobiological) was performed for 1 h at 37 °C before the addition of furin. For negative control, the same buffer was used without furin. The lysis buffer 50 mM Tris, 1% SDS at pH 7.5 was then added, and samples were processed for Western blot analysis as described earlier.

MERS-CoV Internalization Analysis. To track the processing of S during MERS-CoV internalization in cells, 1.2×10^6 MRC-5 cells were plated in 35-mm dishes and incubated at 37 °C for 24 h. The cells were either left untreated or treated with NH_4Cl (5 or 20 μM) for 2 h, placed on ice and washed with PBS, and then MERS-CoV viral supernatant (10^6 $TCID_{50}$/mL) was added. The virus was left to bind for 1 h on ice and then washed with PBS to remove unbound particles. Cells in the binding plate were lysed using 50 mM Tris, 1% SDS at pH 7.5. Internalization plates were placed at 37 °C to allow for internalization to occur. At 10, 30, 60, and 90 min after the start of internalization, the cells were lysed (90 min in the case of NH_4Cl-treated samples and their controls). All samples were then analyzed by Western blot as described earlier.

Immunofluorescence Analyses. Five to 7.5×10^4 Huh-7, MRC-5, WI-38, Vero, MDCK, or primary NHBE were seeded in microscopy chamber slides (Ibidi) and incubated for 24 h at 37 °C (48 h for NHBE). Cells were subjected to treatment with increasing concentrations of dec-RVKR-CMK furin inhibitor for 2 h before infection. MERS-CoV or influenza virus strain A/WSN/1933(H1N1) were used to infect cells at an multiplicity of infection of 10 and 1, respectively. At 8 h postinfection (24 h for NHBE), cells were washed with PBS and fixed for 1 h with 4% paraformaldehyde. The cells were then permeabilized with Triton X-100, blocked with normal goat serum, and immunolabeled for either MERS-CoV S (40069-RP02, SinoBiological) or influenza nucleoprotein (NP; H16-L10-4R5 mouse mAb; American Type Culture Collection), followed by DAPI nuclear staining. The slides were analyzed by microscopy, using an Axiovert 200 microscope (Zeiss) equipped with a SensiCam CCD camera (Cooke). For quantification of percentage of infected cells, images of randomly selected fields (10× objective) per condition were acquired and processed to count the total number of cells (DAPI nuclear stain), and the number of S or NP-positive (infected) cells, using Imaris 6 software analysis (BitPlane). For each condition, a minimum of 2,400 cells were analyzed.

Analysis of MERS-CoV S-Induced Syncytia Formation in Huh-7 Cells. Huh-7 cells were either infected with MERS-CoV for 8 h as described in *SI Immunofluorescence Analyses* or transfected with plasmids encoding wt, S1/S2 mutant, or S2′ mutant MERS-CoV S for 48 h. The transfected cells were nontreated, treated with 75 μM furin inhibitor, or treated with 75 μM furin inhibitor for 24 h, followed by replacement of the inhibitor in medium by exogenous recombinant furin (New England Biolabs). Both infected and transfected cells were processed for immunofluorescence microscopy analysis, as described in *SI Immunofluorescence Analyses*, with acquisition of images performed using a 20× objective. To quantify the extent of syncytia formation, for each condition, 10 syncytia were analyzed for the number of nuclei they contained, and the average number of nuclei/syncytium was calculated.

Statistical Analyses. Experimental data were analyzed and charts plotted using Prism 6 (GraphPad). For statistical significance analysis, two-tailed Student *t* test or, for dose–response experiments, one-way ANOVA test were used. To describe the *P* value significance, the following convention was used: not significant (n.s.), $P > 0.05$; significant (*), $P \leq 0.05$; highly significant (**), $P \leq 0.01$; and very highly significant (***), $P \leq 0.001$.

1. Sun X, Tse LV, Ferguson AD, Whittaker GR (2010) Modifications to the hemagglutinin cleavage site control the virulence of a neurotropic H1N1 influenza virus. *J Virol* 84(17): 8683–8690.
2. Tian S, Huajun W, Wu J (2012) Computational prediction of furin cleavage sites by a hybrid method and understanding mechanism underlying diseases. *Sci Rep* 2:261.
3. Bartosch B, Dubuisson J, Cosset FL (2003) Infectious hepatitis C virus pseudo-particles containing functional E1-E2 envelope protein complexes. *J Exp Med* 197(5):633–642.
4. Livak KJ, Schmittgen TD (2001) Analysis of relative gene expression data using real-time quantitative PCR and the 2(-Delta Delta C(T)) Method. *Methods* 25(4):402–408.

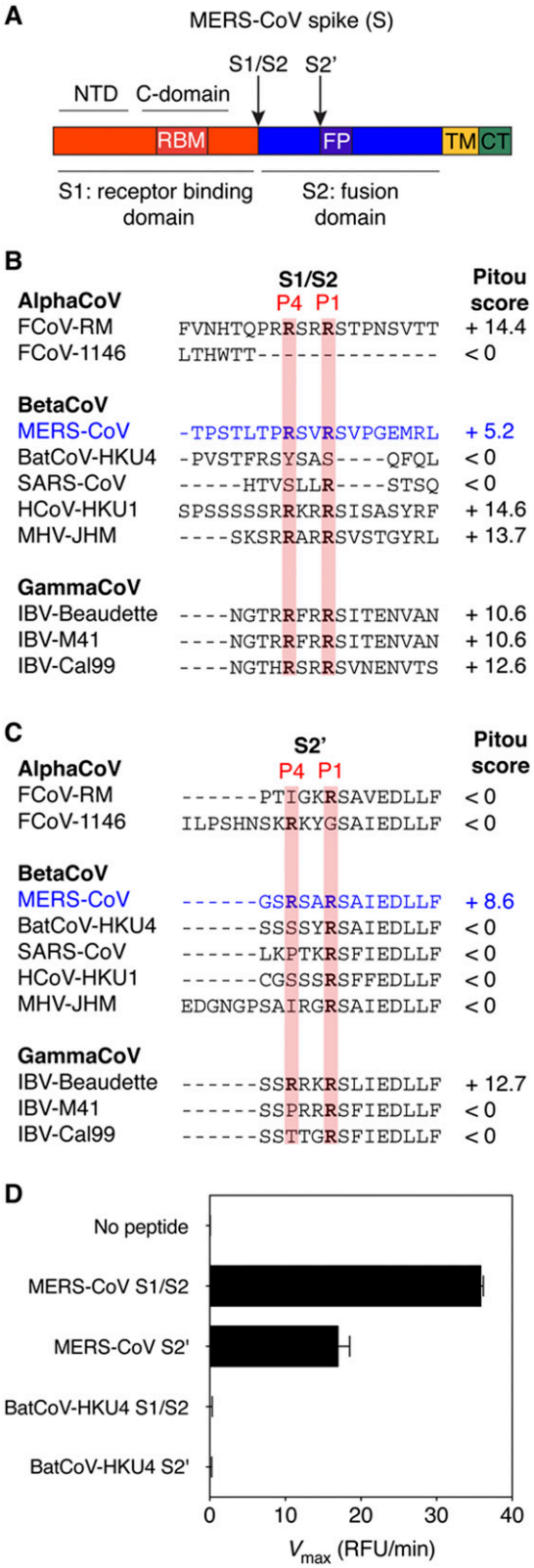

Fig. S1. Characterization of MERS-CoV S S1/S2 and S2′ sites. (*A*) Schematic of MERS-CoV S protein. NTD, N-terminal domain; RBM, receptor-binding motif; FP, fusion peptide; TM, transmembrane domain; CT, C-terminal endodomain. Not drawn to scale. Protein sequence alignment and furin cleavage prediction scores of coronavirus S S1/S2 (*B*) and S2′ sites (*C*). Protein sequences of coronavirus S S1/S2 and S2′ sites were aligned, with the key P1 and P4 positions within furin cleavage sites highlighted. The PiTou 2.0 furin cleavage prediction scores are shown on the right for each sequence, with a positive score indicating predicted furin cleavage and a negative score indicating that furin-mediated cleavage was not predicted. (*D*) Furin proteolytic processing of MERS-CoV S S1/S2 and S2′ fluorogenic peptide mimetics. Fluorogenic peptides with residues matching the S1/S2 and S2′ sites of MERS-CoV and BatCoV-HKU4 S proteins were subjected to treatment with recombinant human furin, and reactions were monitored by fluorometric analysis. Results are expressed as the V_{max} of cleavage reactions with error bars representing SD from the mean ($n = 3$).

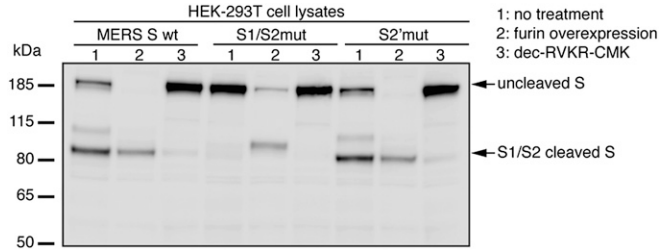

Fig. S2. Furin proteolytic processing during biosynthesis of MERS-CoV S protein in cell lysates. HEK-293T cells, nontreated (1), overexpressing furin (2), or treated with dec-RVKR-CMK furin inhibitor (3), were transiently transfected to express MERS-CoV wt, S1/S2 mutant, or S2′ mutant S, and lysed, and samples were analyzed by Western blot using an anti-S antibody. Arrows denote major S bands observed.

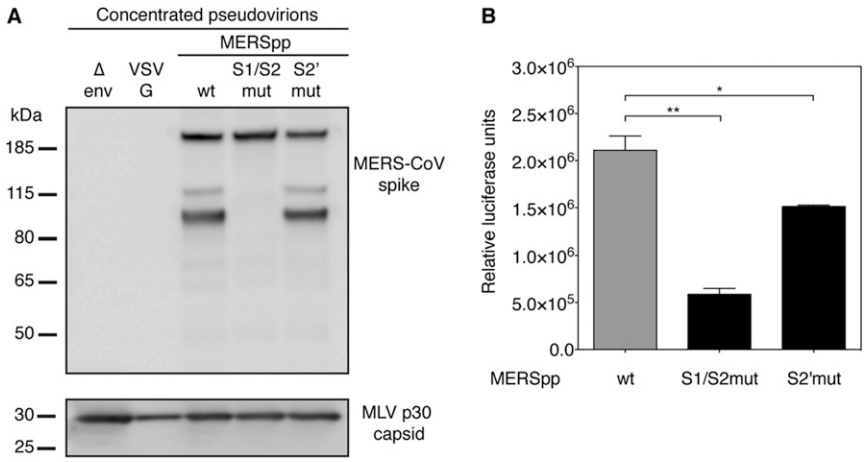

Fig. S3. MERS-CoV wt, S1/S2 mutant, and S2′ mutant S incorporation into MLV pseudovirions and infectivity in Huh-7 cells. (*A*) Incorporation of wt and mutant MERS-CoV S into pseudotyped particles. MLV pseudovirions produced with no envelope glycoprotein (Δenv), the vesicular stomatitis virus (VSV) G protein, wt, S1/S2 mutant, or S2′ mutant MERS-CoV S (MERSpp) were ultracentrifuged, resuspended in PBS, and analyzed by Western blot. For each sample, MERS-CoV S and MLV capsid p30 protein content were analyzed using an antibody against MERS-CoV S and a mouse monoclonal anti-MLV capsid p30, respectively. (*B*) Infectivity of wt and mutant MERSpp. Huh-7 cells were infected with wt, S1/S2 mutant, or S2′ mutant MERSpp. Seventy-two hours postinfection, cells were lysed and luciferase activity was measured. Results are expressed as RLU with error bars representing SD from the mean ($n = 3$). Data were analyzed using two-tailed Student *t* test. *P* value significance: significant (*), $P \leq 0.05$; highly significant (**), $P \leq 0.01$.

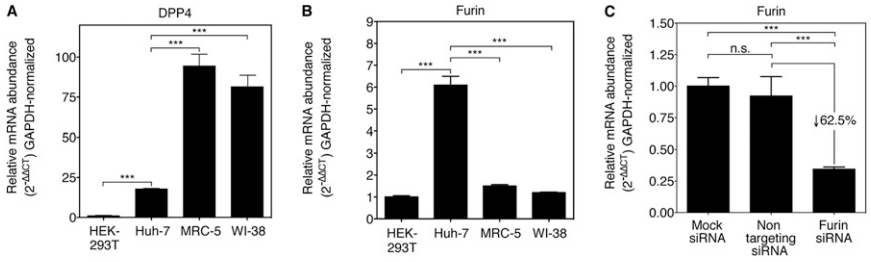

Fig. S4. Quantitative RT-PCR analysis of DPP4 and furin transcripts. Quantification of DPP4 (*A*) and furin (*B*) mRNA levels in different cell lines. Total RNA from HEK-293T, Huh-7, MRC-5, and WI-38 cells were extracted, and one-step quantitative RT-PCR was performed to quantify relative levels of DPP4 (*A*) and furin (*B*) mRNAs for each sample. (*C*) Quantification of siRNA knock-down of furin expression. Total RNA from mock or siRNA-transfected HEK-293T cells were extracted, and one-step quantitative RT-PCR was performed to quantify relative levels of furin mRNA. For *A*, *B*, and *C*, results are expressed as $2^{-\Delta\Delta CT}$ values normalized to GAPDH and standardized to values measured in HEK-293T cells, with error bars representing SD from the mean ($n = 4$). Data were analyzed using two-tailed Student *t* test. *P* value significance: not significant (n.s.), $P > 0.05$; very highly significant (***), $P \leq 0.001$.

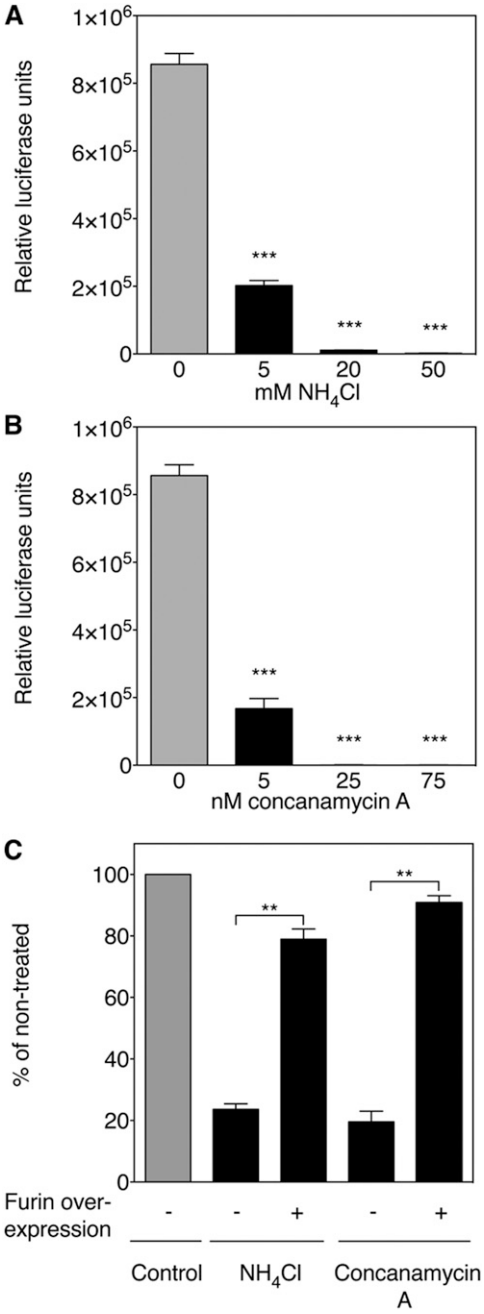

Fig. S5. Role of furin in low pH-dependent MERS-CoV entry. Effect of NH_4Cl (*A*) and the V-ATPase inhibitor concanamycin A (*B*) on MERS-CoV S-mediated entry. HEK-293T cells transiently expressing DPP4 were pretreated with increasing concentrations of NH_4Cl (0–50 mM) or concanamycin A (0–75 nM) and infected with wt MERSpp. (*C*) Effect of enhanced furin expression on low-pH-dependent MERS-CoV entry. HEK-293T cells were transfected with DPP4-encoding plasmid with (+) or without (–) cotransfection of a furin expression plasmid. The cells were then either nontreated or pretreated with NH_4Cl (5 mM) or concanamycin A (5 nM) for 2 h and infected with MERSpp. For *A*, *B*, and *C*, 72 h postinfection, cells were lysed and luciferase activity was measured. Results are expressed as RLU for *A* and *B*, and as percentage of nontreated control for *C*, with error bars representing SD from the mean ($n = 3$). Data were analyzed using one-way ANOVA test for *A* and *B* and two-tailed Student *t* test for *C*. *P* value significance: highly significant (**), $P \leq 0.01$; very highly significant (***), $P \leq 0.001$.

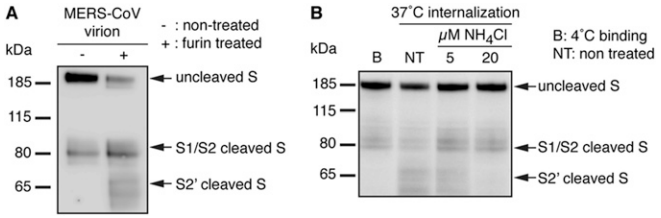

Fig. S6. Furin proteolytic processing of S protein on MERS-CoV virions and role of intracellular pH in generating furin-mediated S2′ cleavage product during internalization. (*A*) Furin-mediated cleavage of S on MERS-CoV virions. MERS-CoV virions from viral supernatants were subjected (+) or not (–) to recombinant human furin treatment. Samples were analyzed by Western blot, using an anti-S antibody. Arrows denote major S bands observed. (*B*) Role intracellular pH in the generation of S2′ furin-mediated cleaved product. MRC-5 cells were treated or not with 5 or 20 μM NH_4Cl for 2 h. MERS-CoV virions were bound to the surface of MRC-5 cells at 4 °C for 1 h. Unbound virions were washed and cells were either lysed or incubated for 90 min at 37 °C to allow internalization of virions and then lysed. B, binding. Samples were analyzed by Western blot using an anti-S antibody. Arrows denote major S bands observed.

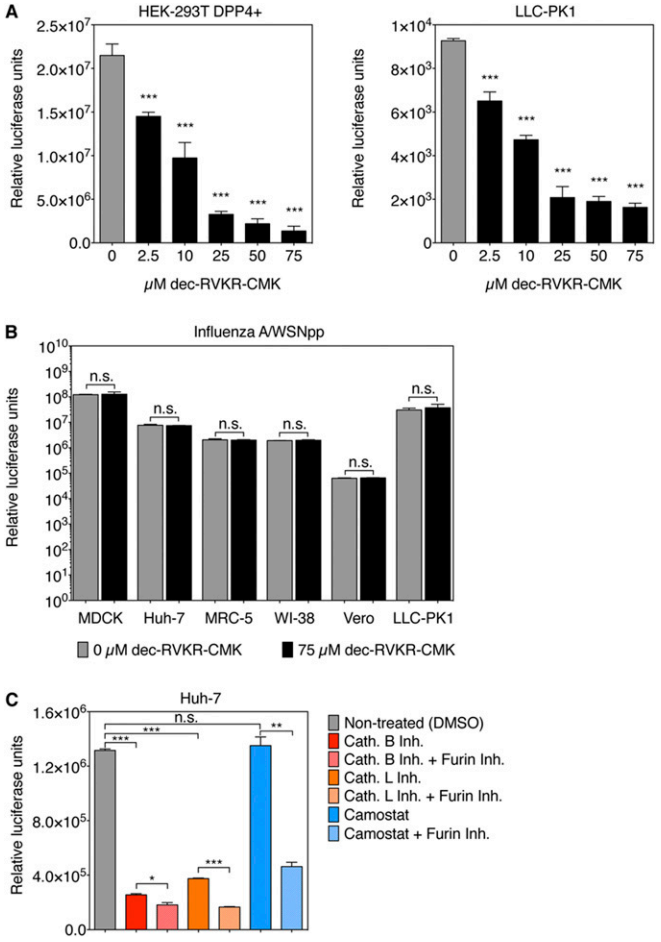

Fig. S7. Effect of host cell protease inhibition on MERS-CoV S-mediated and influenza HA-mediated entry. (*A*) Effect of furin blockade on MERSpp entry. Human HEK-293T overexpressing DPP4 and swine LLC-PK1 cells were pretreated for 2 h with the furin inhibitor dec-RVKR-CMK at increasing concentrations (0–75 μM). The cells were then infected with wt MERSpp. (*B*) Effect of furin blockade on influenza HApp entry. MDCK, Huh-7, MRC-5, WI-38, Vero, and LLC-PK1 cells were treated or not with 75 μM furin inhibitor dec-RVKR-CMK for 2 h. The cells were infected with influenza A/WSN/1933(H1N1) pseudovirions. (*C*) Effect of inhibition of cathepsin B, L, TMPRSS protease, and furin on MERSpp entry in Huh-7 cells. Huh-7 cells were pretreated for 2 h with 25 μM of cathepsin B, L, or camostat (TMPRSS inhibitor), alone or in combination with 25 μM furin inhibitor. The cells were then infected with wt MERSpp. For *A*, *B*, and *C*, 72 h post-infection, cells were lysed and luciferase activity was measured. Results are expressed as RLU with error bars representing SD from the mean ($n = 3$). Data were analyzed using one-way ANOVA test (*A*) or two-tailed Student *t* test (*B* and *C*). *P* value significance: not significant (n.s.), $P > 0.05$; significant (*), $P \leq 0.05$; highly significant (**), $P \leq 0.01$; and very highly significant (***), $P \leq 0.001$.

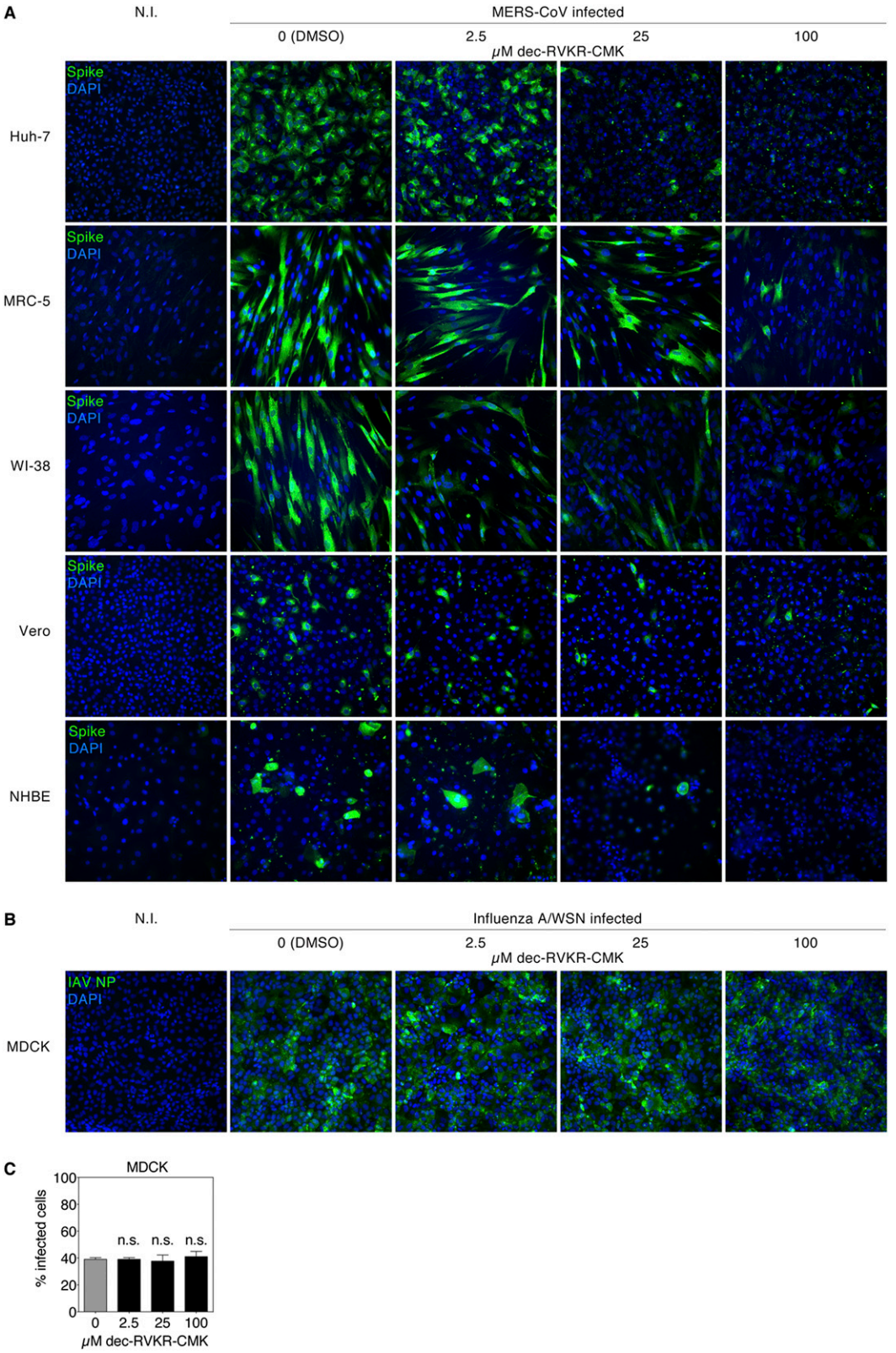

Fig. S8. Effect of furin inhibition on MERS-CoV and influenza virus infection. (*A*) Immunofluorescence assay of MERS-CoV infected cells treated with dec-RVKR-CMK furin inhibitor. Huh-7, MRC-5, WI-38, Vero, and primary NHBE cells were pretreated with increasing concentrations of the furin inhibitor dec-RVKR-CMK (0–100 μM) for 2 h. The cells were infected with MERS-CoV at an m.o.i. of 10 for 8 h (24 h for NHBE). The cells were fixed and immunolabeled for MERS-CoV S and stained for nuclei (DAPI). Cells were analyzed by microscopy, and images were acquired for each condition using a 20× objective. N.I., noninfected. (*B*) Immunofluorescence assay of influenza A virus infected cells pretreated with dec-RVKR-CMK furin inhibitor. MDCK cells were pretreated with dec-RVKR-CMK (0–100 μM) as in *A*. Cells were infected with influenza virus strain A/WSN/1933(H1N1) at an m.o.i. of 1 for 8 h. Cells were analyzed

Legend continued on following page

by microscopy as described in *A*, using a viral NP staining. (*C*) Quantification of influenza virus infected cells. Images of five 10× objective fields were randomly acquired per condition and analyzed for total number of cells (DAPI nuclei stain) and NP-positive cells (infected cells). Results are expressed as percentage infected cells, with error bars representing SD from the mean ($n = 5$). Data were analyzed using one-way ANOVA test. *P* value significance: not significant (n.s.), $P > 0.05$.

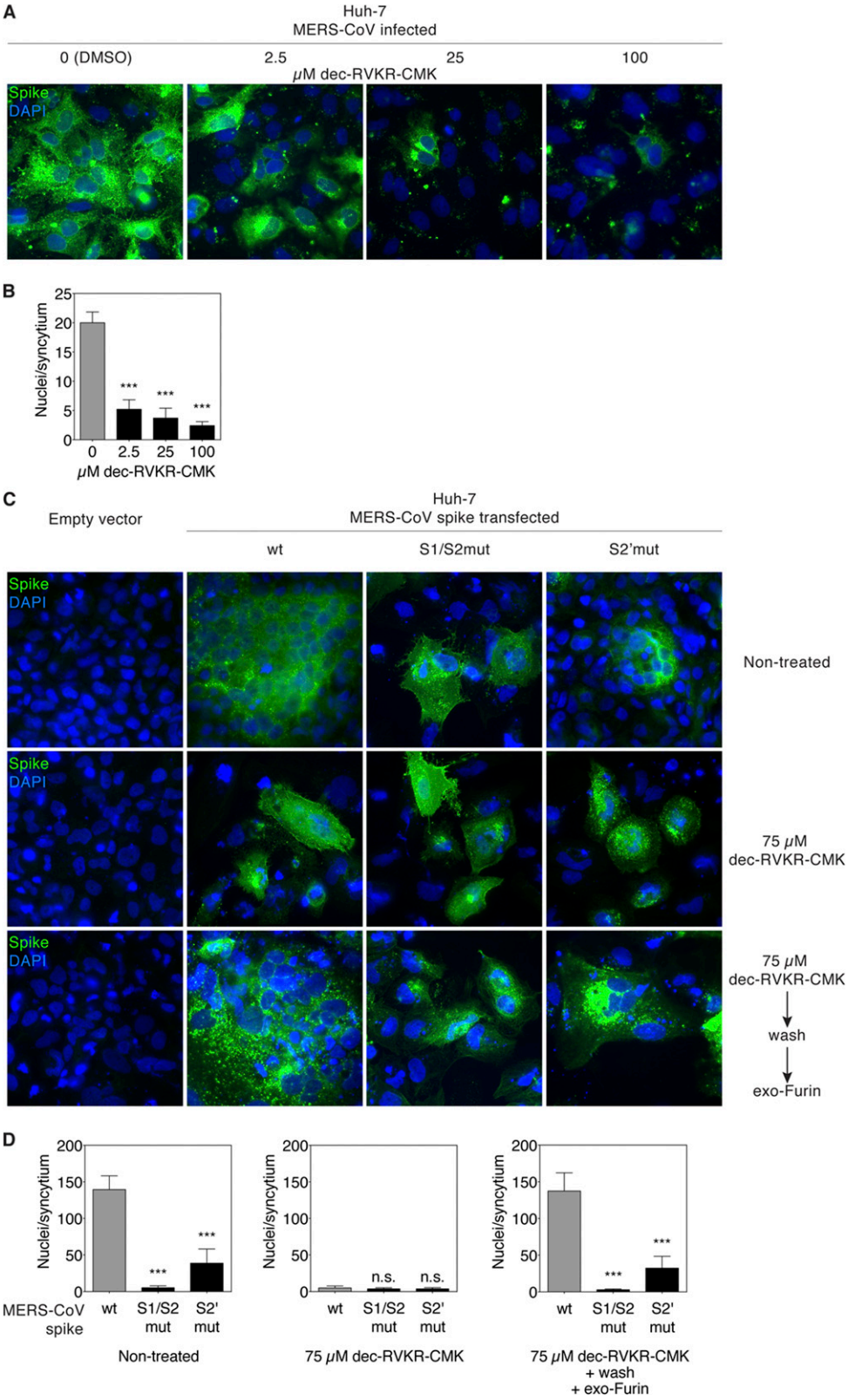

Fig. S9. Role of furin in MERS-CoV S-induced cell–cell fusion activation. (*A*) Analysis of cell–cell fusion in MERS-CoV-infected Huh-7 cells. The cells were infected with MERS-CoV in the presence of increasing concentrations of furin inhibitor and were processed for immunofluorescence microscopy, as described previously. For each condition, images of syncytia present were acquired using a 20× objective. (*B*) Quantification of size of syncytia. For each condition, 10 syncytia were analyzed and the number of nuclei for each syncytium was counted. (*C*) Analysis of cell–cell fusion in Huh-7 cells expressing MERS-CoV S. Huh-7 cells were transfected to express wt, S1/S2 mutant, or S2′ mutant MERS-CoV S. The cells were nontreated, treated with 75 μM furin inhibitor, or treated with 75 μM furin inhibitor for 24 h, followed by replacement of the inhibitor with medium containing recombinant human furin. The cells were fixed 48 h

Legend continued on following page

posttransfection and processed for immunofluorescence microscopy, as in *A*. (*D*) Quantification of size of syncytia. For each condition, 10 syncytia were analyzed and the number of nuclei for each syncytium was counted. Results are expressed as the average number of nuclei per syncytium, with error bars representing SD from the mean ($n = 10$). Data were analyzed using one-way ANOVA test for *B* or two-tailed Student *t* test for *D*. *P* value significance: not significant (n.s.), $P > 0.05$; very highly significant (***), $P \leq 0.001$.

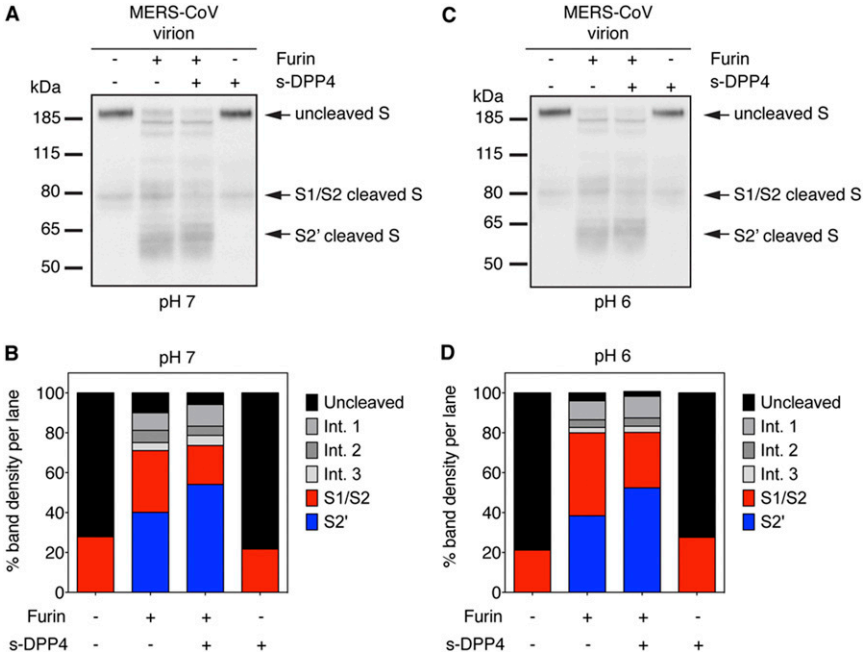

Fig. S10. Role of DPP4 and low pH on furin cleavage activation of MERS-CoV S. (*A*) Western blot analysis of MERS-CoV virions incubated with s-DPP4 and treated with furin at neutral pH. MERS-CoV virions from viral supernatants were incubated or not with s-DPP4 for 1 h at 37 °C. Furin was then added or not, and samples were incubated at 37 °C. Samples were analyzed by Western blot, using an anti-S antibody. Arrows denote major S bands observed. (*B*) Quantification of percentage of S cleavage at neutral pH. For each lane, densitometry analysis was performed using ImageJ. The band densities for each cleavage product were divided by the band densities of all S products (cleaved and uncleaved) for each lane, enabling calculation of percentage density for each band per lane. Int. 1, 2 and 3 designate intermediate bands observed for furin-cleaved samples. (*C*) Western blot analysis of MERS-CoV virions incubated with s-DPP4 and treated with furin at pH 6. Experiment was performed as in *A*, under the slightly acidic condition of pH 6. (*D*) Quantification of percentage of S cleavage at pH 6. The analysis was performed as in *B*, using data from pH 6 condition.